Modeling of the fouling of inside-out hollow fiber UF membranes

Xudong Wang, Danxi Huang, Lei Wang, Xiaorong Meng, Yongtao Lv and Siqing Xia

ABSTRACT

Membrane processes often experience a decline in the permeate flux or an increase in the operating pressure from membrane fouling. A mathematical model that describes the fouling of inside-out hollow fiber ultrafiltration (UF) membranes was derived from hydrodynamic equations coupled with the theory of depth filtration. The correlation predictions obtained in this study are simpler, as the effect of membrane characteristics, water recovery, and membrane washing processes on UF membrane fouling were expressed using a single parameter: the membrane blocking coefficient. Membrane filtration tests were conducted using diluted paper industry wastewater in a constant-pressure and constant-current operational mode. The effects of different operating conditions, such as water recovery and cleaning methods, and membrane characteristics, on the membrane blocking coefficient were evaluated. The predictive capability of the proposed model was excellent, according to a comparison of the experimental results and model simulations.

Key words | hollow fiber membrane, inside-out, mathematical model, membrane fouling, ultrafiltration

Xudong Wang
Danxi Huang
Lei Wang (corresponding author)
Yongtao Lv
Siqing Xia
School of Environmental & Municipal Engineering,
Xi'an University of Architecture and Technology,
Yan Ta Road. No.13,
Xi'an 710055,
China
E-mail: wl0178@126.com

Xiaorong Meng
School of Science,
Xi'an University of Architecture and Technology,
Yan Ta Road. No.13, Xi'an 710055,
China

Siqing Xia
College of Environmental Science and Engineering,
Tongji University,
Shanghai 200092,
China

LIST OF SYMBOLS

x the distance from the inlet to the specific position, m
p the lumen-side pressure at the x position, m
p_1 the inside pressures of the hollow fiber membrane, m
p_2 the lumen-side pressure in the membrane inlet, m.
p_3 the outside pressures of the hollow fiber membrane, m
D the effective internal diameters, m
L membrane length, m
g acceleration of gravity, m/s^2
u flux, m/s
$\bar{u}$ average permeation velocity, m/h
r a constant and named membrane plugging coefficient, s/m^2
k_0 the initial permeation coefficient
k the process permeation coefficient

GREEK LETTERS

σ the ratio of irreversible fouling to pore volume

ρ the water density, kg/m^3
v flow velocity inside the fiber , m/s
μ kinetic viscosity coefficient of water, cP
ε_0 the initial membrane porosity, %
ε the process membrane porosity, %
β the constant

INTRODUCTION

The extremely high packing density of their fibers and the presence of specially designed channels confer hollow fiber membrane modules with excellent mass-transfer properties and higher water permeability, which have led to numerous commercial applications in various fields. Because of the flexibility of hollow fiber membranes, they can be used to carry out filtration using inside-out,

outside-in, or dead-end patterns, according to the required filtration and influent quality targets.

However, the wide use of hollow fiber membrane technology has been hampered by membrane fouling, which causes a decrease in permeate flux and increase in membrane pressure, and which shortens membrane lifetimes. There are several possible causes of membrane fouling, which depend on various factors, for example, the properties of the membrane (membrane morphology, charge, and hydrophobicity) (Kumar & Ulbricht 2014; Li *et al.* 2014; Kumar & Ismail 2015; Sinha & Purkait 2015), type of solute used (molecular weight (MW) (Qi *et al.* 2012), log Kow, and pKa), feed water characteristics (concentration, ion strength, and pH) (Sweity *et al.* 2011; Gao *et al.* 2012; Miao *et al.* 2015), and operating conditions used (pressure, temperature, crossflow rate, and backwash interval) (Sim *et al.* 2011; Raffin *et al.* 2012), as well as effects from interactions between the membrane, solute, and solvent (Adhikara *et al.* 2013; Lei *et al.* 2013; Tao *et al.* 2014).

For the efficient application of these modules and to prolong their lifetimes, an accurate assessment of membrane fouling, a realistic optimization of the operating conditions, and an effective strategy for membrane cleaning are necessary, despite the high antifouling performance of the hollow fiber membranes. Many researchers have focused on dynamic analysis and simulations of fouling processes under different operating conditions, which is very important in saving time and energy for the effective control of membrane fouling.

Membrane ultrafiltration (UF) processes have been analyzed using the gel polarization model, osmotic pressure model, resistance-in-series model, and balance equations (Fane 1984; Nabetani *et al.* 1990; Huang & Morrissey 1998; Song 1998). Hermia *et al.* introduced four types of membrane fouling mechanisms: complete blocking, intermediate blocking, standard blocking, and cake filtration. This model was valid for an unstirred, dead-end filtration mode (Hermia 1982). Huang *et al.* proposed a unified membrane fouling index based on the Hermia model to quantify and assess the fouling of low-pressure membranes observed under both constant-pressure and constant-flux filtration (Huang *et al.* 2007). Yeh *et al.* developed a modified correlation equation for predicting the permeate flux of UF membranes in hollow fiber modules derived from the complete momentum balance coupled with the application of an exponential model (Yeh 2009). Yuriy *et al.* developed a mathematical model using a dead-end outside-in hollow fiber membrane filter (Polyakov 2006). Liu *et al.* proposed a filtration model for membrane fouling during crossflow UF (Wei *et al.* 2005). Yoon *et al.* has developed pressure drop models for hollow fiber membranes (Yoon *et al.* 2008).

All these mathematical models of membrane fouling can be placed into two main categories. The first is exponential empirical models, which can achieve perfect correspondence with the experimental results, but are only associated with a few impact factors and so are non-universal. The physical meaning of each parameter is not clear, and such models fail to explain theoretically the phenomenon of membrane fouling. The second is phenomenal fouling models that describe fouling according to the changes in membrane properties. The parameters in such models have an exact physical meaning, but their complexity limits their practical application.

Usually, the extent of membrane fouling is assessed from the flux decline ratio, water recovery, and membrane fouling resistance. It has been shown that different types of fouling can exist with irreversible, reversible, and even similar flux decline ratios. Therefore, Wang *et al.* proposed a membrane structure parameter model to describe the reduction in mean pore size and pore density depending on the flux based on hydrodynamic theory, and to some extent, this model better reflected the UF membrane filtration process data (Wang & Wang 2006). However, this model neglected the effect of rejection on membrane fouling. Fujita has developed a model to simulate the effect of membrane blocking in outside-in hollow fiber membranes with the flux and volume of accumulated fouling particles (Kenji 1995).

Based on the Fujita model, in this paper, a mathematical model for describing the fouling of inside-out hollow fiber UF membranes is derived from hydrodynamic equations coupled with the theory of depth filtration. The effects of membrane characteristics, feed water properties, and the membrane washing process, as well as other factors, on UF membrane fouling are expressed using a single parameter: the membrane blocking coefficient. Membrane filtration tests were conducted using diluted paper industry wastewater in a constant-pressure operation mode, and the effects of different operating conditions, such as water

recovery and cleaning methods, and membrane characteristics, on the membrane blocking coefficient were evaluated. The correlation predictions obtained in this study are simpler than those obtained in previous work.

MATHEMATICAL MODEL

Pressure drop inside a hollow fiber

In an inside-out hollow fiber membrane, liquid permeates through the membrane from the inside to the outside, resulting in a drop in pressure inside the hollow fiber, as shown in Figure 1.

Traditionally, hollow fiber membrane modules are designed to have a low aspect ratio (diameter to length) in order to achieve a high packing density (surface area per unit module volume) and to prevent collapse of the fiber during pressure-driven filtration. Carroll *et al.* found that a high internal pressure drop has important consequences for the fouling of these membranes (Carroll & Booker 2000). The change in internal pressure along the length of the hollow-fiber membrane leads to an axially dependent flux through the membrane wall, which impacts on the degree of fouling (Decarolis *et al.* 2001). These axial features play an important role in both the rate and mechanism of fouling during the initial and intermediate stages of fouling, and the decrease in the permeate flow rate is dominated by these axial features until substantial fouling has occurred.

Therefore, the problem of dealing with the pressure distribution can be approached by setting up an energy conversion equation within the differential length, dx, of a hollow fiber. During steady-state operation (Altmann &

Figure 1 │ Flow and pressure drop in an inside-out hollow fiber UF membrane.

Ripperger 1997):

$$p + \frac{v^2}{2g} = p - dp + \frac{(v - dv)^2}{2g} + \frac{32\mu v}{gD^2\rho}dx, \tag{1}$$

For laminar flow, the term $(dv)^2$ can be neglected, and the above equation can be rewritten as:

$$dp = -\frac{v}{g}dv + \frac{32\mu v}{gD^2\rho}dx, \tag{2}$$

where x is the distance from the inlet to the specific position, (m); p denotes the lumen-side pressure at the x position (m); D is the effective internal diameter (m); v is flow velocity inside the fiber (m/s); ρ is the water density (kg/m^3); g is the acceleration due to gravity (m/s^2); and μ is the kinetic viscosity coefficient of water (cP).

The pressure drop inside a hollow fiber can be calculated using Equation (3), where the decrement flow rate in an infinitesimal block of fiber is equal to the volume of water permeated in the same block.

$$\frac{\pi}{4}D^2dv = \pi Dudx, \tag{3}$$

This equation can be rearranged to form Equation (4):

$$\frac{dv}{dx} = \frac{4}{D}u = a_1 u, \tag{4}$$

where u is the flux, in m/s, and $a_1 = 4/D$.

For laminar flow, the flux can be assumed to be proportional to the transmembrane pressure (TMP), and can be described using the following equation:

$$u = k(p_1 - p_3), \tag{5}$$

where k is the permeability constant, and P_3 and P_1 are the outside and inside pressures of the hollow fiber membrane, respectively. Substituting Equations (4) and (5) into Equation (2), we have:

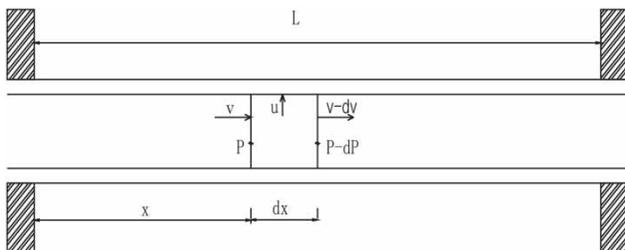$$\frac{dp}{dv} = -\frac{v}{g}\left[1 - \frac{8\mu}{D\rho k(p_1 - p_3)}\right], \tag{6}$$

In Equation (6), because item 1 is much less than item 2, we can neglect item 1, to obtain:

$$\frac{dp}{dv} = \frac{8\mu v}{\rho g D k (p_1 - p_3)}, \tag{7}$$

Substitution of Equations (4) and (5) into Equation (7) yields:

$$\frac{dp}{dx} = \frac{32\mu v}{\rho g D^2} = a_2 v, \tag{8}$$

where $a_2 = 32\mu/(\rho g D^2)$.

Relationship between membrane fouling and the permeability constant, *k*

Assumptions regarding membrane fouling

Membrane fouling can be classified as reversible or irreversible, according to the degree of foulant removal after hydraulic backwashing. Irreversible fouling is mainly related to the amount of foulant adsorbed in the membrane pores. Therefore, the following assumptions were made in the development of our analysis:

(1) All the dissolved organic matter retained in the membrane pore that cannot be removed by hydraulic backwashing is likely to lead to irreversible fouling.
(2) The volume of accumulated fouling particles at the x position at unit time, σ, is proportional to the TMP at the specified position:

$$\frac{d\sigma}{dt} \propto p_1 - p_3. \tag{9}$$

(3) σ is proportional to the flux at the specified position:

$$\frac{d\sigma}{dt} \propto u. \tag{10}$$

(4) σ is inversely proportional to the number of retained particles, i.e., the effective membrane porosity. When $\sigma = 0$,

then $\varepsilon_0 = 1$, and when $\sigma = \varepsilon_0$, then $\varepsilon = 0$:

$$\frac{d\sigma}{dt} \propto 1 - \frac{\sigma}{\varepsilon_0}, \tag{11}$$

On integrating Equations (9)–(11), and (5), we obtain:

$$\frac{d\sigma}{dt} \propto (p_1 - p_3)u\left(1 - \frac{\sigma}{\varepsilon_0}\right) \tag{12}$$

Namely,

$$\frac{d\sigma}{dt} = \beta(p_1 - p_3)u\left(1 - \frac{\sigma}{\varepsilon_0}\right) \tag{13}$$

where β is the constant.

Substitution of Equation (5) into Equation (13) yields:

$$\frac{d\sigma}{dt} = \beta\frac{u}{k}u\left(1 - \frac{\sigma}{\varepsilon_0}\right) = \frac{\beta}{k}u^2\left(1 - \frac{\sigma}{\varepsilon_0}\right) \tag{14}$$

where k is the permeability constant, in order to simplify the parameters, we used r instead of β/k, to obtain:

$$\frac{d\sigma}{dt} = ru^2\left(1 - \frac{\sigma}{\varepsilon_0}\right) \tag{15}$$

where r is a constant with units s/m^2, known as the membrane blocking coefficient, which captures the effects of membrane characteristics, feed water characteristics, and cleaning methods.

Permeability coefficient, *k*

The permeability coefficient, k, is equal to k_0 during the initial filtration stage. However, the permeate flux and the permeability constant will change with the irreversible accumulation of foulant. UF membranes have a thin top layer whose typical structure comprises closely packed polymeric spheres, the so-called nodular structure (nodule size = 20–100 nm), supported by a very open porous layer, often containing large elongated voids called macrovoids. This type of membrane can be optimized to separate colloidal molecules in a low-molecular-weight solute (Smolders *et al.* 1992). The main separation mechanism in the UF process is governed

by steric hindrance (or size exclusion). Therefore, according to traditional filtration theory, the relationship between the head losses, h, and the porosity, ε, can be given as:

$$h \propto \frac{(1-\varepsilon)^2}{\varepsilon^3} u, \tag{16}$$

In the UF process, the TMP drop is as shown in Equation (17):

$$p_1 - p_3 \propto \frac{(1-\varepsilon)^2}{\varepsilon^3} u, \tag{17}$$

Compared with Equation (5):

$$k \propto \frac{\varepsilon^3}{(1-\varepsilon)^2}, \tag{18}$$

where $\varepsilon = \varepsilon_0 - \sigma$.

Assuming that the foulant in the membrane pores is distributed uniformly, then for $\varepsilon = \varepsilon_0 - \sigma$, it can be shown that:

$$\frac{k}{k_0} = \frac{\varepsilon^3 (1-\varepsilon_0)^2}{(1-\varepsilon)^2 \varepsilon_0^3} = \frac{(\varepsilon_0 - \sigma)^3 (1-\varepsilon_0)^2}{(1-\varepsilon_0 + \sigma)^2 \varepsilon_0^3}$$
$$= \frac{(1-\sigma/\varepsilon_0)^3}{[1+\sigma/(1-\varepsilon_0)]^2}, \tag{19}$$

where σ is the ratio of irreversible fouling volume to pore volume, k_0 and k are the initial and process permeation coefficients, respectively, and ε_0 and ε are the initial and process membrane porosities, respectively.

TMP drop

Average permeation velocity

The membrane permeate flow rate decreases with the membrane length, L, and therefore the average permeate flow rate was evaluated from the water flow divided by the membrane area as:

$$\overline{u} = \frac{(v_1 - v_2)D}{4L} = \frac{(v_1 - v_2)}{a_1 L}, \tag{20}$$

where $\bar{u}$ denotes the average permeation velocity, m/h; v_1 is the lumen-side flow rate in the membrane inlet, m/h; v_2 is

the lumen-side flow rate in the membrane outlet, m/h; and L is the membrane length, m.

TMP drop (ΔP)

The decrease in internal pressure along the length of a hollow-fiber membrane leads to an axially dependent flux through the membrane wall. Here, the average pressure, $\overline{p}$, was calculated as:

$$\overline{p} = \frac{p_1 + p_2}{2}, \tag{21}$$

$$\Delta p = \overline{p} - p_3 = \frac{p_1 + p_2}{2} - p_3, \tag{22}$$

$$\Delta p = \frac{\overline{u}}{k}, \tag{23}$$

where P_2 is the lumen-side pressure in the membrane inlet, m.

Establishment of membrane fouling model

A mathematical model for describing the fouling of inside-out hollow fiber UF membranes was derived from hydrodynamic equations coupled with the theory of depth filtration:

This expression for σ was integrated over the operational time ($0 < t < \infty$) using the following boundary conditions:

$$\sigma_{t=0} = 0 \quad \text{and} \quad \sigma_{t=\infty} = \varepsilon_0, \tag{24}$$

Integration of Equation (15) with the boundary conditions above yields:

$$\sigma = \varepsilon_0 - \varepsilon_0 \exp\left(-\frac{ru^2 t}{\varepsilon_0}\right), \tag{25}$$

where t is the operational time. The membrane blocking coefficient, r, can be calculated using Newton's iteration method. Since k_0 can be obtained from Equation (23) according to the initial TMP and permeation velocity, then k can be obtained by the substitution of Equation (25) into Equation (19). On combining this with Equation (23), the relationship between the TMP and the permeation velocity and time can be derived.

MATERIALS AND METHODS

UF fouling experiments were carried out employing polysulfone (PSf, molecular weight cut-off (MWCO) = 100 kDa) and polyacrylonitrile (PAN, MWCO = 30 kDa) hollow fiber membrane modules, using the filtration apparatus shown in Figure 2. The fibers had an internal diameter of 1.3 mm and an external diameter of 1.9 mm, and were 1,016 mm in length. Filtration occurred from the inside to the outside of the fibers. The fibers were wetted and degreased with ethanol, and flushed thoroughly with Milli-Q water. The feed stream was prepared using diluted paper industry wastewater with UV254 = 0.13.

After filtration, chemical cleaning was carried out using the following sequence: an NaOH solution (pH = 12) followed by an NaClO solution (5 mg/L), then hydraulic cleaning using tap water and an NaClO solution (5 mg/L).

RESULTS AND DISCUSSION

Membrane blocking coefficient (*r*) under different operating conditions

The set experimental protocols and the results for the membrane blocking coefficient obtained in the constant-pressure mode are shown in Table 1.
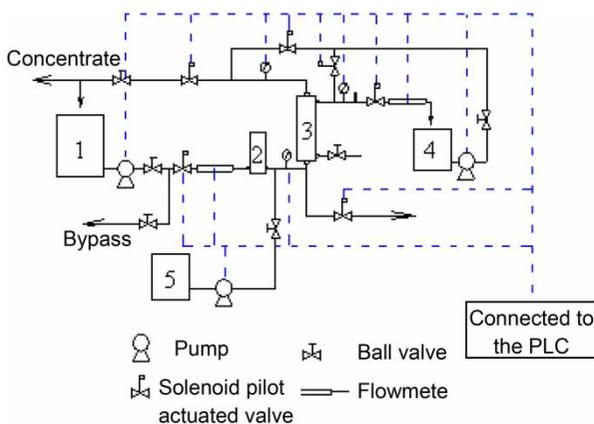
Figure 2 │ The UF membrane system used.

It can be seen that the conditions that led to an increase in membrane fouling also led to an increase in the membrane blocking coefficient, which, to a certain extent, represented the degree of membrane fouling. The membrane cleaning procedure was optimized according to the value of the membrane blocking coefficient.

Effect of water recovery, membrane characteristics, and cleaning on *r* in the constant-pressure mode

#### Effect of type of cleaning and cleaning frequency on the model parameter, *r*

It is usually accepted that the flux decline in aqueous solutions is mainly caused by the adsorption or crystallization of organic and inorganic foulants, possibly enhanced by pore blocking and/or cake formation. Thus, effective membrane cleaning plays an important part in eliminating membrane fouling. Membrane cleaning involves hydraulic and chemical cleaning to remove reversible and irreversible membrane fouling, respectively. Different cleaning modes have different applications (Al-Amoudi & Lovitt 2007). For example, acid cleaning is suitable for the removal of precipitated salts, such as $CaCO_3$, while alkaline cleaning is employed extensively for adsorbed organics. Particulates and colloids can only be removed by hydraulic cleaning. Hydraulic cleaning methods are often adopted in UF for drinking water treatment to achieve a water recovery between 50% and 80%, owing to the dominant rejection mechanism of steric hindrance. Four types of hydraulic cleaning have been developed: forward flushing, backwashing, forward flushing followed by backwashing, and backwashing followed by forward flushing. In this study, several combined washing methods were investigated, as shown in Table 1 and Figure 3.

The value of *r* simulated using MATLAB procedures is shown for each of these cleaning modes, respectively: 6,498, 6,637, 6,791, and 7,142 s/m^2 (Table 1). According to Equation (22), higher values of r will lead to more severe membrane fouling. This study on the hydraulic cleaning of fouled UF membranes shows the following:

(1) Backwashing is more effective than forward flushing. However, a single hydraulic cleaning mode could not

Table 1 │ Effect of membrane characteristics, water recovery, and cleaning methods on the membrane blocking coefficient (r) in the constant-pressure operating mode

Membrane material	Cleaning frequency	TMP (kPa)	Backwashing pressure (kPa)	Forward flushing pressure (kPa)	water recovery (R_W)	r (s/m²)
PSf	60 min	30	50 (90 s)	16 (30 s)	80%	3,737
PSf	60 min	30	50 (90 s)	16 (30 s)	100%	4,531
PSf	30 min	30	50 (90 s)	16 (30 s)	80%	4,552
PAN	30 min	30	50 (90 s)	16 (30 s)	80%	2,167
Cleaning type and cleaning duration						
Protocol 1: backwashing 90 s + forward flushing 30 s						6,498
Protocol 2: forward flushing 30 s + backwashing 90 s + forward flushing 30 s						6,637
Protocol 3: backwashing 30 s						6,791
Protocol 4: forward flushing 30 s						7,142
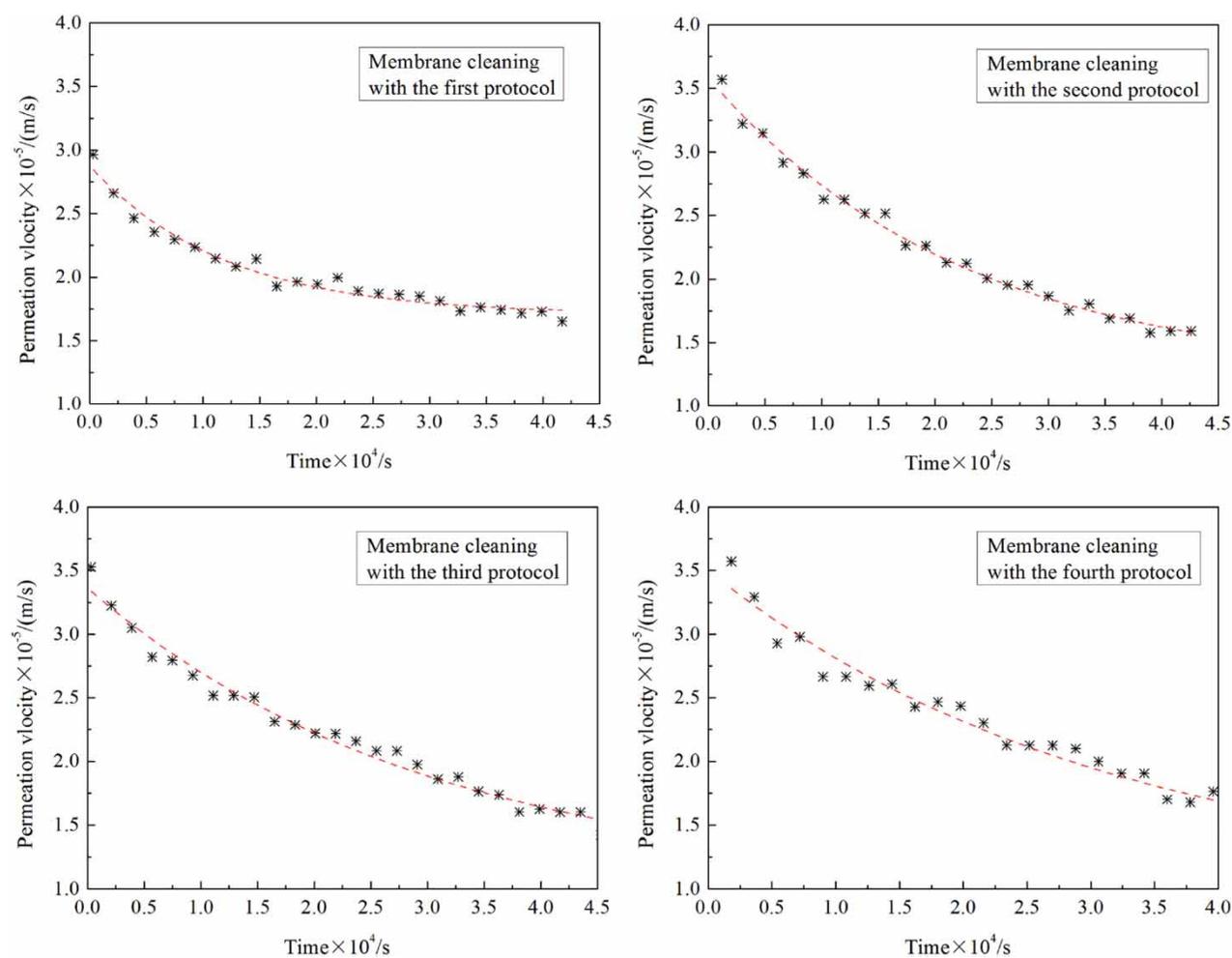
Figure 3 │ A comparison of the fits to the experimental permeation velocity using models with different membrane cleaning modes and frequencies in a constant-pressure operating mode with PSf membranes.

satisfy the needs of water recovery (the third and the fourth cleaning protocols in Table 1 and Figure 3).

(2) A combined mode using backwashing (90 s) followed by forward flushing (30 s) was the most effective mode for removing membrane fouling, with the smallest value of r (the first cleaning protocol in Table 1 and Figure 3). Liang *et al.* also found that backwashing followed by forward flushing was more effective for water recovery, and that a 20 min duration was long enough to achieve cleaning (Liang *et al.* 2008). Perhaps this is because backwashing disturbs any foulant deposited on the membrane surface, and the debris is flushed out by the following forward flushing process. In addition, using a combined washing process is more water efficient than using a single washing process. In another study, backwashing followed by a forward flushing was applied during cleaning.

(3) The effect of the second cleaning protocol was less pronounced. This could be because the initial forward flushing only partly removes the foulant, and some of the removed foulant is flushed into the internal pores and can become somewhat compacted. The first cleaning protocol is more effective.

(4) It was also found that hydraulic cleaning alone could not effectively remove UF membrane fouling from diluted paper industry wastewater, and therefore, effective chemical cleaning is necessary to detach different classes of foulants from the membrane to restore its permeate flux characteristics.

Effect of water recovery on the model parameter, *r*

The water recovery ($R_w = Q_p/Q_F$, where Q_p and Q_F are the permeate and feed volumetric flow rates, respectively) is inversely proportional to the crossflow velocity. When the water recovery is low, the crossflow velocity is high. The permeate flux increases linearly with increasing crossflow velocity. In addition, at a high crossflow velocity, particles cannot be easily deposited onto the membrane surface (Choi *et al.* 2005). However, Wang and Fukushi observed that membrane foulants are likely to result from the combined effects of particle size and water recovery (Wang & Fukushi 2003). On decreasing the water recovery, the MW of the foulant increases and a porous layer is formed. By contrast, when the MW of the foulant decreases, a denser layer forms. In this study, water recoveries of 80% and 100% were investigated. A comparison of the fits obtained to the experimental permeation velocity is shown in Figure 4, using a model with different flux recoveries in the constant-pressure mode ($\Delta P = 30$ kPa (3.06 mH_2O), PSf UF membrane, filtration frequency = 60 min, and forward flushing pressure = 16 kPa).

It has been reported that a reversible fouling layer is likely to result from the combined effects of membrane pore size, particle size, and fluid mechanics. Here, the membrane pore size and the foulant properties are similar, so the main influencing factor is the water recovery. It is known that a strong turbulent flow in the membrane channels is
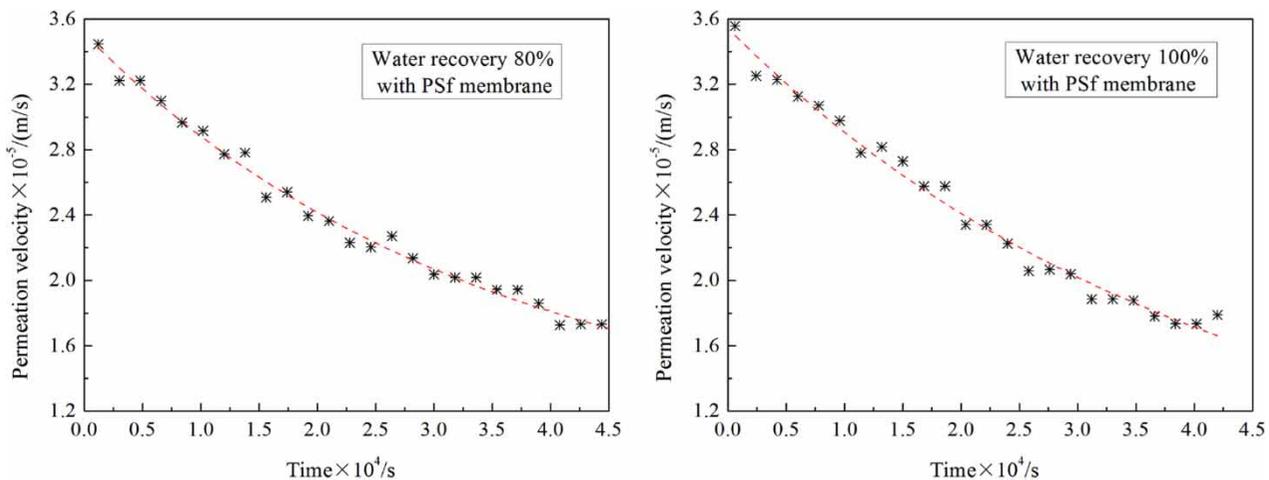
Figure 4 │ A comparison of the fits obtained to the experimental permeation velocity using a model with different flux recoveries in the constant-pressure mode ($\Delta P = 30$ kPa (3.06 mH_2O), PSf UF membrane, filtration frequency = 60 min, and forward flushing pressure = 16 kPa).

effective in reducing membrane fouling. Under laminar flow, fluid particles move along definite and observable paths or streamlines, resulting in a change in momentum without mixing. However, in turbulent flow, fluid particles between the streamlines exchange their momenta vigorously and randomly over a brief time interval, resulting in disturbance of the fouling layer and a reduction in membrane fouling.

On increasing the water recovery from 80% to 100%, the membrane blocking coefficient, r, increases from 3,737 to 4,531 s/m^2, as calculated using a MATLAB procedure. Crossflow membrane filtration can decrease the membrane blocking coefficient about 1.2 times more than dead-end filtration can. As a result, low water recovery is more effective in reducing fouling because of the high flow velocity. Filtration resistance caused by a concentration in polarization and a reversible fouling layer significantly decreases with decreasing water recovery because of a high shear force. It is also shown in Figure 4 that the membrane blocking coefficient, r, is effective for determining the extent of membrane fouling, even though the flux decline is near identical.

Effect of membrane characteristics on the model parameter, *r*

Figure 5 shows a comparison of the fits obtained to the experimental permeation velocity using a model with different membrane characteristics in the constant-pressure mode

(ΔP = 30 kPa, filtration frequency = 30 min, backwashing pressure = 50 kPa (90 s), forward flushing pressure = 16 kPa (30 s), and water recovery = 80%). The MWCOs of the selected PSf and PAN hollow fiber UF membranes were 100 kDa and 30 kDa, respectively. In principle, the larger the membrane pore size, the higher the value of the pure water flux. However, the profile of the permeation velocity versus the operating time was similar for the different membranes, while the membrane blocking coefficient, r, differed greatly, with r = 4,552 s/m^2 for PSf and r = 2,167 s/m^2 for PAN, as calculated using a MATLAB procedure. Long & Hawkes (2007) observed that membrane fouling was more severe for larger pore sizes or higher initial fluxes, compared with smaller-pore-size membranes or lower initial fluxes because of the tendency toward irreversible fouling for larger-pore-size membranes from adsorption and membrane pore blocking. Choi *et al.* (2005) also found that large particles, such as suspended solids in biological suspensions, may be more easily deposited onto microfiltration (MF) membranes than UF membranes at high flux recoveries because of the larger size of the MF membrane pores.

The MWCO of the PSf membrane was greater than that of the PAN membrane, and the PAN membrane had a higher degree of hydrophilicity than the PSf membrane. As a result, considering the larger pores of the PSf membrane, it is hypothesized that this membrane required a higher crossflow velocity to prevent reversible fouling than the PAN membrane did. Under the same conditions, the PSf
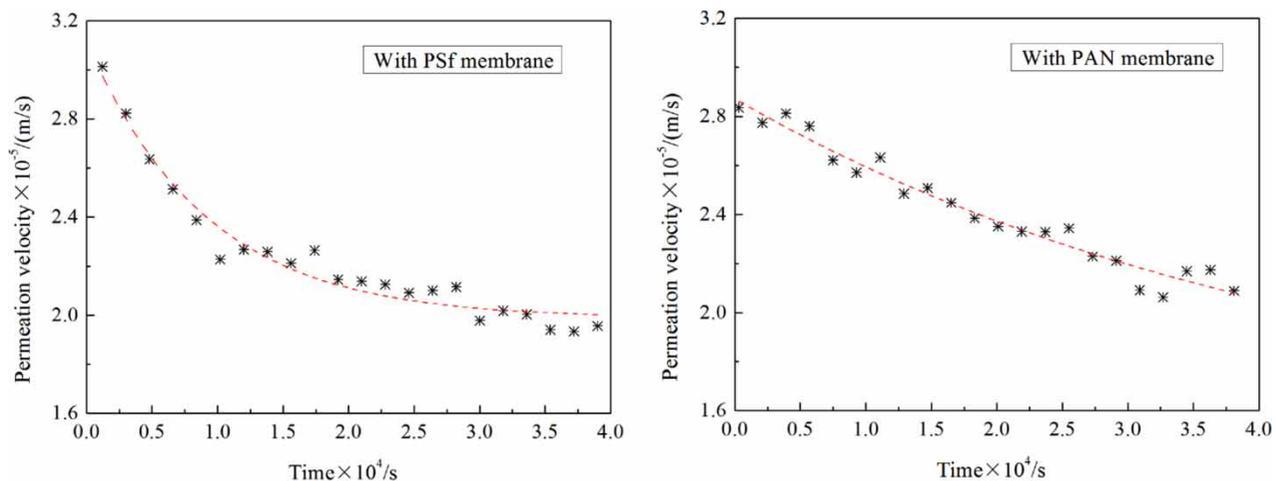
Figure 5 | A comparison of the fits to the experimental permeation velocity using a model with different membrane characteristics in the constant-pressure mode (ΔP = 30 kPa, filtration frequency = 30 min, backwashing pressure = 50 kPa (90 s), forward flushing pressure = 16 kPa (30 s), and water recovery = 80%).

membrane fouled more easily than the PAN membrane did. This result is consistent with other published reports. Comparing the r values listed in Table 1, the PAN membrane resisted fouling better than the PSf membrane did because of its higher hydrophilicity.

CONCLUSIONS

The correlation predictions obtained in this study are simple, as the effects of membrane characteristics, water recovery, and the membrane cleaning process on hollow fiber UF membrane fouling are expressed using a single parameter: the membrane blocking coefficient, r. The following was found:

(1) The conditions that can lead to an increase in membrane fouling will increase the value of r, which, to a certain extent, represents membrane fouling. The value of r is an effective metric to determine the extent of membrane fouling, even though the flux decline is nearly identical.

(2) Low water recovery is more effective in reducing fouling because of a high flow velocity, and crossflow membrane filtration can decrease the membrane blocking coefficient by about 1.2 times more than dead-end filtration can.

(3) Backwashing is more effective than forward flushing. However, the combined washing methods investigated were the most effective at removing membrane fouling, with the smallest values of r. The effect of the second cleaning protocol was less than that of the first cleaning protocol. It was also found that hydraulic cleaning alone could not effectively remove UF membrane fouling from diluted paper industry wastewater, and therefore, effective chemical cleaning was necessary. It is important to avoid membrane fouling through better pretreatment, and this allows more feasible and cost-effective cleaning and performance restoration procedures.

ACKNOWLEDGEMENTS

REFERENCES

Adhikara, R., Yun, Y., Pierre, L. C. & Vicki, C. 2013 Analysis of UF membrane fouling mechanisms caused by organic interactions in seawater. *Water Research* **47** (2), 911–921.

Al-Amoudi, A. & Lovitt, R. W. 2007 Fouling strategies and the cleaning system of NF membranes and factors affecting cleaning efficiency. *Journal of Membrane Science* **303** (1–2), 4–28.

Altmann, J. & Ripperger, S. 1997 Particle deposition and layer formation at the crossflow microfiltration. *Journal of Membrane Science* **124** (1), 119–128.

Carroll, T. & Booker, N. A. 2000 Axial features in the fouling of hollow-fibre membranes. *Journal of Membrane Science* **168** (1–2), 203–212.

Choi, H., Zhang, K., Dionysiou, D. D., Oerther, D. B. & Sorial, G. A. 2005 Influence of cross-flow velocity on membrane performance during filtration of biological suspension. *Journal of Membrane Science* **248** (1–2), 189–199.

Decarolis, J., Hong, S. & Taylor, J. 2001 Fouling behavior of a pilot scale inside-out hollow fiber UF membrane during dead-end filtration of tertiary wastewater. *Journal of Membrane Science* **191** (1–2), 165–178.

Fane, A. G. 1984 Ultrafiltration of suspensions. *Journal of Membrane Science* **20** (3), 249–259.

Gao, Y., Chen, D., Weavers, L. K. & Walker, H. W. 2012 Ultrasonic control of UF membrane fouling by natural waters: effects of calcium, pH, and fractionated natural organic matter. *Journal of Membrane Sciences* **401–402** (10), 232–240.

Hermia, J. 1982 Constant pressure blocking filtration law: application to powder-law non-Newtonian fluid. *Trans. Inst. Chem. Eng.* **60**, 183–187.

Huang, L. & Morrissey, M. T. 1998 Fouling of membranes during microfiltration of surimi wash water: roles of pore blocking and surface cake formation. *Journal of Membrane Science* **144** (1–2), 113–123.

Huang, H., Young, T. A. & Jacangelo, J. G. 2007 Unified membrane fouling index for low pressure membrane filtration of natural waters: principles and methodology. *Environmental Science & Technology* **42** (3), 714–720.

Kenji, F. 1995 A filtration model for outside-in hollow fiber membranes. In: *Conference Proceeding of MAC21-Related Research*, Tap Water Purification Process Association, Tokyo, Japan, pp. 13–29.

Kumar, M. & Ulbricht, M. 2014 Low fouling negatively charged hybrid ultrafiltration membranes for protein separation from

sulfonated poly(arylene ether sulfone) block copolymer and functionalized multiwalled carbon nanotubes. *Separation & Purification Technology* **127** (1), 181–191.

Kumar, R. & Ismail, A. F. 2015 Fouling control on microfiltration/ultrafiltration membranes: effects of morphology, hydrophilicity, and charge. *Journal of Applied Polymer Science* **132** (21), 42042.

Lei, W., Rui, M., Xudong, W., Yongtao, L., Xiaorong, M., Yongzhe, Y., Danxi, H., Ling, F., Ziwen, L. & Kai, J. 2013 Fouling behavior of typical organic foulants in polyvinylidene fluoride ultrafiltration membranes: characterization from microforces. *Environ. Sci. Technol* **47** (8), 3708–3714.

Li, F., Meng, J., Ye, J., Yang, B., Tian, Q. & Deng, C. 2014 Surface modification of PES ultrafiltration membrane by polydopamine coating and poly(ethylene glycol) grafting: morphology, stability, and anti-fouling. *Desalination* **344**, 422–430.

Liang, H., Gong, W., Chen, J. & Li, G. 2008 Cleaning of fouled ultrafiltration (UF) membrane by algae during reservoir water treatment. *Desalination* **220** (1–3), 267–272.

Long, D. N. & Hawkes, S. 2007 Effects of membrane fouling on the nanofiltration of pharmaceutically active compounds (PhACs): Mechanisms and role of membrane pore size. *Separation & Purification Technology* **57** (1), 176–84.

Miao, R., Wang, L., Mi, N., Gao, Z., Liu, T., Lv, Y., Wang, X., Meng, X. & Yang, Y. 2015 Enhancement and mitigation mechanisms of protein fouling of ultrafiltration membranes under different ionic strengths. *Environmental Science & Technology* **49**, 6574–6580.

Nabetani, H., Nakajima, M., Watanabe, A., Nakao, S.-I. & Kimura, S. 1990 Effects of osmotic pressure and adsorption on ultrafiltration of ovalbumin. *AIChE Journal* **36** (6), 907–915.

Polyakov, Y. S. 2006 Deadend outside-in hollow fiber membrane filter: mathematical model. *Journal of Membrane Science* **279** (1–2), 615–624.

Qi, L., Wang, H. C. & Li, G. B. 2012 Effects of natural organic matters molecular weight distribution on the immersed ultrafiltration membrane fouling of different materials. *Desalination & Water Treatment* **50** (1), 95–101.

Raffin, M., Germain, E. & Judd, S. J. 2012 Influence of backwashing, flux and temperature on microfiltration for wastewater reuse. *Separation & Purification Technology* **96** (33), 147–153.

Sim, L. N., Yun, Y., Chen, V. & Fane, A. G. 2011 Comparison of MFI-UF constant pressure, MFI-UF constant flux and Crossflow Sampler-Modified Fouling Index Ultrafiltration (CFS-MFI$_{UF}$). *Water Research* **45** (4), 1639–1650.

Sinha, M. K. & Purkait, M. K. 2015 Preparation of fouling resistant PSF flat sheet UF membrane using amphiphilic polyurethane macromolecules. *Desalination* **355**, 155–168.

Smolders, C. A., Reuvers, A. J., Boom, R. M. & Wienk, I. M. 1992 Microstructures in phase-inversion membranes. Part 1. Formation of macrovoids. *Journal of Membrane Science* **73** (2–3), 259–275.

Song, L. 1998 A new model for the calculation of the limiting flux in ultrafiltration. *Journal of Membrane Science* **144** (1–2), 173–185.

Sweity, A., Wang, Y., Belfer, S., Oron, G. & Herzberg, M. 2011 pH effects on the adherence and fouling propensity of extracellular polymeric substances in a membrane bioreactor. *Journal of Membrane Science* **378** (s 1–2), 186–193.

Tao, L., Shen, B., Wei, C. & Zhang, X. B. 2014 Interaction mechanisms associated with organic colloid fouling of ultrafiltration membrane in a drinking water treatment system. *Desalination* **332** (1), 100–108.

Wang, L. & Fukushi, K. I. 2003 Experimental research on influences of NF performance by the apparent molecular weight distributions of organic pollutants in water. *Water & Wastewater Engineering* **29** (7), 35–37.

Wang, L. & Wang, X. 2006 Study of membrane morphology by microscopic image analysis and membrane structure parameter model. *Journal of Membrane Science* **283** (1–2), 109–115.

Wei, L., Zuoxiang, Z., Weilan, X. & Yali, Y. 2005 A filtration model for membrane fouling during crossflow ultrafiltration. *Journal of East China University of Science and Technology (Natural Science Edition)* **31** (5), 589–592.

Yeh, H. M. 2009 Exponential model analysis of permeate flux for ultrafiltration in hollow-fiber modules by momentum balance. *Chemical Engineering Journal* **147** (2–3), 202–209.

Yoon, S.-H., Lee, S. & Yeom, I.-T. 2008 Experimental verification of pressure drop models in hollow fiber membrane. *Journal of Membrane Science* **310** (1–2), 7–12.